Interconnection between microstructure and microhardness of directionally solidified binary Al-6wt.%Cu and multicomponent Al-6wt.%Cu-8wt.%Si alloys

ANGELA J. VASCONCELOS[1], RAFAEL H. KIKUCHI[2], ANDRÉ S. BARROS[1], THIAGO A. COSTA[1],
MARCELINO DIAS[1], ANTONIO L. MOREIRA[1], ADRINA P. SILVA[1] and OTÁVIO L. ROCHA[1,2]

[1]Faculdade de Engenharia Mecânica, Universidade Federal do Pará, Avenida Augusto Corrêa, 1, 66075-110 Belém, PA, Brasil
[2]Instituto Federal de Educação, Ciência e Tecnologia do Pará, Avenida Almirante Barroso, 1155, 66093-020 Belém, PA, Brasil

ABSTRACT

An experimental study has been carried out to evaluate the microstructural and microhardness evolution on the directionally solidified binary Al-Cu and multicomponent Al-Cu-Si alloys and the influence of Si alloying. For this purpose specimens of Al-6wt.%Cu and Al-6wt.%Cu-8wt.%Si alloys were prepared and directionally solidified under transient conditions of heat extraction. A water-cooled horizontal directional solidification device was applied. A comprehensive characterization is performed including experimental dendrite tip growth rates (V_L) and cooling rates (T_R) by measuring Vickers microhardness (HV), optical microscopy and scanning electron microscopy with microanalysis performed by energy dispersive spectrometry (SEM-EDS). The results show, for both studied alloys, the increasing of T_R and V_L reduced the primary dendrite arm spacing (λ_1) increasing the microhardness. Furthermore, the incorporation of Si in Al-6wt.%Cu alloy to form the Al-6wt.%Cu-8wt.%Si alloy influenced significantly the microstructure and consequently the microhardness but did not affect the primary dendritic growth law. An analysis on the formation of the columnar to equiaxed transition (CET) is also performed and the results show that the occurrence of CET is not sharp, i.e., the CET in both cases occurs in a zone rather than in a parallel plane to the chill wall, where both columnar and equiaxed grains are be able to exist.

Key words: solidification, metals and alloys, electron microscopy, hardness.

INTRODUCTION

Cast aluminum alloys yield cost-effective products due to the low melting point, although they generally have lower tensile strengths than wrought alloys. These alloys are widely used in engineering structures and components where light weight or corrosion resistance is required (Rooy 1990). Alloys composed mostly of aluminum have been very important in aerospace manufacturing since the introduction of metal skinned aircraft. In this context, a car manufacturing process now includes aluminum as engine castings, wheels, radiators and increasingly as body parts (Haro et al. 2009, Polmear 2006, Rooy 1990). Among the most widely used aluminum casting alloys are those that contain silicon and copper with different amounts. Copper contributes to strengthening and machinability, and the silicon is necessary to incorporate, in the eutectic matrix of Al-Cu alloys, sufficient quantities

Correspondence to: Otávio Fernandes Lima da Rocha
E-mail: otvrocha@oi.com.br

of hard primary silicon particles to provide high wear resistance (Polmear 2006).

We highlight the Al-Cu-Si alloy system which is of great importance in the die casting industry. In these alloys the addition of Cu increases considerably the strength of Al-Si alloys due to precipitation of Al_2Cu intermetallic phase ($q^{'}$) dispersed in the Al-rich dendritic matrix during ageing (Emma and Salem 2010). In the case of adding Si to Al-Cu alloys fluidity is promoted because of the high heat of fusion for silicon (1810 kJ/kg compared with 395 kJ/kg and 205 kJ/kg for aluminum and cooper, respectively) which increases "fluid life" (i.e., the distance the molten alloy can flow in a mold before being too cold to flow further) (Polmear 2006). However, machining may present difficulties because of the presence of hard silicon particles in the microstructure. Other advantages of the presence of Si in these alloys are the increased corrosion resistance and weldability. It is observed that Al-Cu-Si alloys with higher values of Si are used for pressure die castings, whereas alloys with lower silicon and higher copper are used for sand and permanent mold castings (Polmear 2006).

The microstructure of aluminum components mainly depends on the casting process and thermal parameters, such as solidification rate (Goulard et al. 2010) but chemical composition obviously also has a significant effect on the mechanical properties (Gomes et al. 2015). In this sense, the process parameters during solidification affect the microstructural development of the alloy and consequently the final engineering performance of the casting. Dendrite arm spacings, segregation patterns, nature, size, distribution and morphology of precipitates and porosity all affect final mechanical properties.

Studies on the transient solidification of ternary alloys relating microstructural parameters and their correlations with mechanical properties have been developed in the literature (Atwood and Lee 2003, Costa et al. 2015, Ferreira et al. 2010, Sadrossadat

and Johansson 2010, Swaminathan and Voller 1997, Voller 1998). The vast majority has been developed for vertical upward directional solidification (Easton et al. 2010, Ferreira et al. 2010, Rappaz and Boettinger 1999, Sadrossadat and Johansson 2010, Swaminathan and Voller 1997, Voller 1998). In the case of vertical upward directional solidification, the influence of the convection is minimized when solute is rejected for the interdendritic regions, providing the formation of an interdendritic liquid denser than the global volume of liquid metal. On the other hand, in the horizontal unidirectional solidification, when the chill is placed on the side of the mold, the convection as a function of the composition gradients in the liquid always occurs once in this configuration act simultaneously the gradient of density and solute concentration in a vertical direction. Moreover, there will also be a vertical temperature gradient in the sample as soon as a thermosolutal convection roll emerges. In spite of these particular physical characteristics, only a few studies have reported these important effects of melt convection and direction of growth on dendrite arm spacings for this particular case (Carvalho et al. 2013, Costa et al. 2015, Quaresma et al. 2000, Silva et al. 2009, 2011).

The main objective of this work is to investigate the influence of the addition of silicon in a binary Al-Cu (Al-6wt.%Cu) alloy for the development of the microstructure of a ternary alloy (Al-6wt.%Cu-8wt.%Si) and its corresponding effect on the microhardness. A comparative study considering the microstructures and microhardness profiles of examined alloys is performed.

MATERIALS AND METHODS

SAMPLES PREPARATION AND SOLIDIFICATION

Experiments on directional solidification (DS) were performed with the Al-6wt.%Cu and Al-6wt.%Cu-8wt.%Si alloys in a horizontal water-cooled furnace with heat being extracted directionally by one of

the side walls. The experimental casting assembly applied to achieve directional solidification of investigated alloys, shown schematically in Figure 1a, was designed at the Federal Institute of Education, Science and Technology of Pará, Brazil, and it was recently published in previous articles (Carvalho et al. 2013, Costa et al. 2015, Silva et al. 2009, 2011). It was manufactured in such a way that the heat was extracted only through the water-cooled system placed in the lateral mold wall, promoting horizontal directional solidification. The carbon steel mold used had a wall thickness of 3 mm, a length of 110 mm, a height of 60 mm and a width of 70 mm. The lateral inner mold surfaces were covered with a layer of insulating alumina and the upper part of the mold was closed with refractory material to prevent heat losses. The thermal contact condition at the metal/mold interface was also standardized with the heat-extracting surface being polished.

The alloys were melted *in situ* and heated until a superheat of 10% above the *liquidus* temperature (T_L) using an electrical furnace. Approaching the superheat temperature, the mold was taken from the heater and set immediately on a water-cooled carbon steel chill. Water was circulated through this cooling jacket keeping the carbon steel plate during the solidification at a constant temperature of about 25 ºC and thus inducing a longitudinal heat transfer from the mold. Solidification occurred dendritically from the lateral chill surface, forming a columnar structure. During the solidification process, temperatures at different positions in the alloy samples were measured and the data were acquired automatically. For the measurements, a set of five fine type K thermocouples was used. The thermocouples were sheathed in 1.6 mm diameter steel tubes, and positioned at 5, 10, 15, 30, and 50 mm from the heat-extracting surface. The thermocouples were calibrated at the melting point of Al exhibiting fluctuations of about 0.4 ºC, and connected by coaxial cables to a data logger

interfaced with a computer. Previous measurements of the temperature field were carried out confirming that the described experimental set-up fulfills the requirement of a directional heat flow in horizontal direction.

MEASUREMENTS OF GROWTH RATE AND COOLING RATE

It is well known that the primary dendritic arm spacings are dependent on the solidification thermal parameters such as growth rate (V_L) and cooling rate (T_R), all of which vary with time and position during solidification. In order to determine more accurate values of these parameters, the results of experimental thermal analysis have been used to determine the displacement of the *liquidus* isotherm, i.e., the thermocouples readings have also been used to generate a plot of position from the metal/mold interface as a function of time corresponding to the *liquidus* front passing by each thermocouple. The thermocouples readings (Figure 1b) have been used to generate a plot of position from metal/mold interface (P) as a function of time (t) corresponding to the *liquidus* front passing by each thermocouple. A best fitting curve on these experimental points has generated a power function of position as a function of time, i.e., P = f (t). This has been obtained by the Origin 8.0 software. The method has been detailed in recent article (Carvalho et al. 2013). The derivative of this function with respect to time has yielded values for V_L. The T_R profile was calculated by considering the thermal data recorded immediately after the passing of the *liquidus* front by each thermocouple. The method used for measuring the tip cooling rate was detailed by Rocha et al. (2003).

METALLOGRAPHIC ANALYSIS

Each ingot was sectioned along its longitudinal direction, which is parallel to both the sample axis and the direction of solidification. After this, the metallographic specimens were mechanically

polished with abrasive papers and subsequently etched with an acid solution composed of 5 ml of H_2O, 60 ml of HCl, 30 ml of HNO_3 and 5 ml of HF to reveal the macrostructures. A columnar to equiaxed transition (CET) was observed in both cases. The CET positions in the investigated alloys were clearly delineated by visual observation and optical microscopy on the etched surface, and the distances from the side of the samples were measured.

Selected transverse (perpendicular to the growth direction) sections of the directionally solidified specimens at 10, 15, 20, 30, 40, and 50 mm for Al-6wt.%Cu alloy and 5, 10, 15, 20, 30, and 50 mm for Al-6wt.%Cu-8wt.%Si alloy, from the metal/mold interface, were polished and etched with a solution of 5% of NaOH in water for micrograph examination. Image processing system Olympus BX51 and Image Tool (IT) software were used to measure primary arm spacings (about 20 independent readings for each selected position, with the average taken to be the local spacing) and their distribution range. The method used for measuring the primary arm spacing (λ_1) on the transverse section was the triangle method (Çadirli and Gündüz 2000, Rocha et al. 2003).

The triangle occurred by joining the three neighbor dendrite centers and sides of the triangle are corresponded to λ_1. In this method at least 30 primary dendrite spacing were measured for each transverse section.

Moreover, microstructural characterization was performed using a scanning electron microscope (SEM Shimadzu, VEGA 3 SBU TESCAM) coupled to an energy dispersion spectrum (EDS AZTec Energy X-Act, Oxford).

Vickers microhardness measurements in this work were carried out using a Shimadzu HMV-2 hardness measuring test device using a 100 g load and a dwell time of 10 s. The adopted Vickers microhardness was the average of at least 20 measurements on each sample.

RESULTS AND DISCUSSION

Figure 1b shows experimental cooling curves for the five thermocouples inserted into the casting during the solidification of the alloys investigated in this study. The directionally solidified structures of the alloys studied in this work are shown in Figure 2. The macrostructures consisted of elongated columnar grains, aligned approximately parallel to the direction of the heat flow, as well as of equiaxed grains of varying extent and random orientations. It can be observed the formation of a macrostructure composed of two structural zones, featuring a columnar to equiaxed transition (CET) and that approximately fifty percent of the Al-Cu and Al-Cu-Si ingots are composed of a columnar dendritic grain structure, after which it is observed a region of equiaxed dendritic grains. It is also observed, in both ingots that the basic feature of the CET is that the transition is not sharp, i.e., the CET occurs in a zone rather than a plane parallel to the metal/mold interface, where both columnar and equiaxed grains are be able to exist. It can be highlighted that an important feature of the horizontal solidification is the gradient of solute concentration and density in vertical direction, because solute-rich liquid falls down whereas free solvent-crystals rise due buoyancy force. The study of CET is not the main objective of this work. However, the effect of the solidification growth direction in the CET has been investigated in recent article for Al-Cu and Al-Cu-Si alloys (Costa et al. 2015).

Figure 2 presents microstructures of cross sections of samples at 5 and 30 mm from the metal/mold interface, showing the primary dendrite arms. The dendrite arm spacings were sufficiently distinct to make reasonably accurate measurements along the casting length. Experimental laws of power type represented by $\lambda_1 = k_1 (V_L)^{-1.1}$ and $\lambda_1 = k_2 (T_R)^{-0.55}$, were obtained for both alloys studied in this work, where k_1 and k_2 are equal to 57 and 216 for the Al-6wt.%Cu alloy and 92 and 290 for the Al-6wt.%Cu-

1. water inlet; 2. water outlet; 3. insulating ceramic shielding; 4. electric heaters; 5. stainless steel mold; 6. thermocouples; 7. setup cover; 8. temperature controller; 9 and 10. data acquisition system.

(a)

(b)
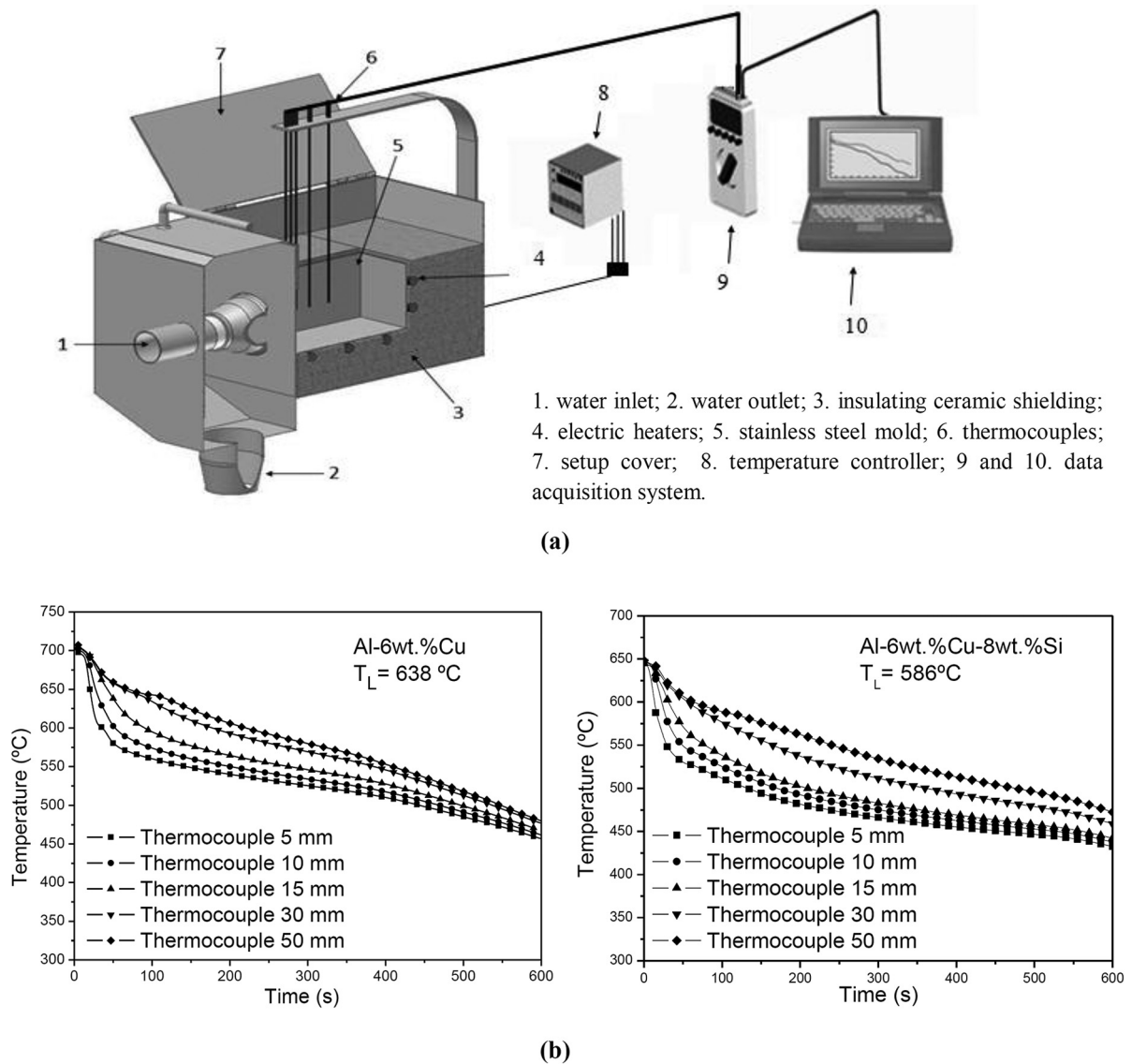
Figure 1 - (**a**) Scheme of the experimental apparatus for horizontal directional solidification and (**b**) Experimental cooling curves for five thermocouples located at different positions from the metal-cooling chamber interface.

8wt.%Si alloy, respectively, which characterize the experimental variation of the primary dendrite arm spacing as a function of growth rate (V_L) and the cooling rate (T_R). It can be seen that the addition of Si in the binary Al-6wt.%Cu alloy did not influence the growth law of primary dendrite arm spacing as a function of V_L and T_R, i.e., the exponents -1.1 and -0.55 for both alloys analyzed in this work are maintained. These results are in agreement with observations reported by Carvalho et al. (2013)

and Rocha et al. (2003) who claim that exponential relationships λ_1 = constant $(V_L)^{-1.1}$ and λ_1 = constant $(T_R)^{-0.55}$ best generate the experimental variation of primary dendritic arms with growth rate and cooling rate along the unsteady-state solidification of binary Al-Si (transient horizontal solidification) and Al-Cu (transient vertical solidification) alloys, respectively. In other recent study (Costa et al. 2015), Al-6wt.%Cu and Al-6wt.%Cu-4wt.%Si alloys were directionally solidified upwards and
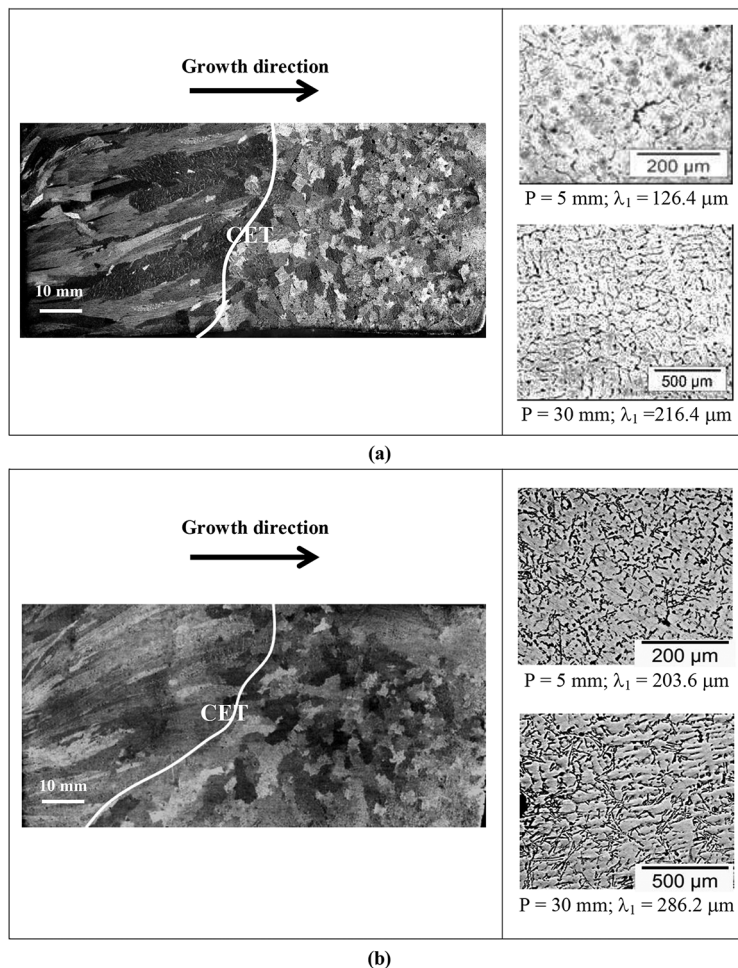
Figure 2 - Solidification microstructures and macrostructures, CET positions, and corresponding primary spacings: (**a**) Al–6wt.%Cu; (**b**) Al-6wt.%Cu-8wt.%Si.

horizontally in transient heat extraction, it was observed that the addition of Si did not affect in experimental growth laws of primary dendrite arm spacing as a function of V_L and T_R, resulting in the same exponents -1.1 and -0.55, respectively, obtained in this work.

Figure 3 shows the dependence of the micro-hardness (HV) with the distance (P) from the metal/ mold interface on primary dendrite arm spacings (λ_1) for the investigated alloys. It can be noted that HV decreases with P and increases for lower values of λ_1 more significantly in the ternary Al-6wt.%Cu-8wt.%Si alloy. It is also observed that the addition of silicon in the binary Al-6wt.%Cu alloy increases

the values of HV, i.e., by fixing a value of P and λ_1 in the graphs of Figure 3a and 3b, respectively, it is observed higher values of HV for the ternary alloy. As it can be seen by Figure 3, the variation of HV on λ_1 can be represented by power type equations given by HV=204$(\lambda_1)^{-0.15}$ and HV=3926$(\lambda_1)^{-0.6}$ for the Al-6wt.%Cu and Al-6wt.%Cu-8wt.%Si alloys, respectively.

It is known from the literature that similar equations were also obtained by Çadirli (2013), Kaya et al. (2008, 2012) and Barros et al. (2015) to investigate the influence of primary dendrite arm spacing on microhardness of Al-based binary alloys. Kaya et al. (2008) have reported that the
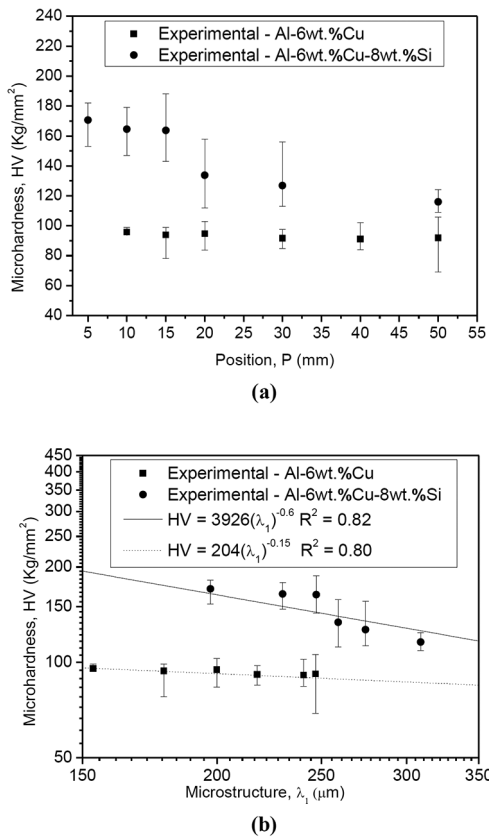
Figure 3 - Microhardness evolution as a function of: (**a**) position in casting, (**b**) the primary dendrite arm sapcing.

power equation proposed in this work is a rewritten form from the traditional equation of Hall-Petch (HP), which has been proposed recently by Çadirli (2013) and Barros et al. (2015), whose authors have established the HV dependence as a function of λ_1 given by the general expression $HV \approx k_i (\lambda_1)^{-n}$, where ki is the Hall-Petch slope, which was determined experimentally for various Al-Cu alloys. The HP-type experimental equations obtained by these authors for Al-Cu alloys are shown in Table I. A comparison with the results of this work is also observed in this table as well as in Figure 4. It is observed that the exponent value of λ_1 obtained for the Al-6wt.%Cu alloy is equal to 0.15, whose value is fairly close to the values of 0.098 and 0.12 obtained by Barros et al. (2015) for Al-Cu alloys in unsteady-state horizontal solidification. On the other hand, considering the works developed for steady-state upward solidification the exponent values 0.29, 0.23, 0.25, and 0.25 obtained by Çadirli (2013) for Al_{100-x}-Cu_x alloys (x=3 wt%, 6 wt%, 15 wt%, 24 wt%) are approximately two time larger than the value of 0.15 of this work, except for the

TABLE I

Hall-Petch experimental expressions proposed in this work of microhardness as a function of the primary dendrite arm spacings and comparison with other from the literature for Al-Cu alloys.

Alloy	Unstady-state horizontal solidification	Steady-state upward solidification
Al-3wt.%Cu	$HV = 97(\lambda_1)^{-0.098}$ (Barros et al. 2015)	$HV = 525.2(\lambda_1)^{-0.40}$ (Kaya et al. 2008) $HV = 307.6(\lambda_1)^{-0.29}$ (Çadirli 2013)
Al-6wt.%Cu	$HV = 204(\lambda_1)^{-0.15}$ (This work)	$HV = 344.3(\lambda_1)^{-0.23}$ (Çadirli 2013)
Al-8wt.%Cu	$HV = 151(\lambda_1)^{-0.12}$ (Barros et al. 2015)	-
Al-15wt.%Cu	-	$HV = 680.4(\lambda_1)^{-0.25}$ (Çadirli 2013)
Al-24wt.%Cu	-	$HV = 810.9(\lambda_1)^{-0.25}$ (Çadirli 2013)
Al-33wt.%Cu	-	$HV = 331(l_E)^{-0.19}$ (Çadirli 2013)
Al-6wt.%Cu-8wt.%Si	$HV = 3926(\lambda_1)^{-0.6}$ (This work)	-

value obtained for the alloy Al-33wt.%Cu, which was equal to this work (0.15), and the value of 0.4 obtained by Kaya et al. (2008) is approximately three times this value (0.15).

It is known that there is no literature HP-type expressions of HV = f (λ_1) for Al-Cu-Si alloys. However, it is possible to observe in Table I that the slope value of 3926, obtained for the ternary Al-Cu-Si alloy studied in this work, is much higher than the values obtained by Kaya et al. (2008), Çadirli (2013) and Barros et al. (2015) for binary Al-Cu alloys. The exponent value of 0.6 is also higher than the exponents obtained for Al-Cu alloys. Figure 4 shows a comparison between HP-type experimental curves obtained in this study with the literature. It can be seen that the Si in the Al-Cu-Si alloy has produced higher HV values, compared to the values obtained for binary Al-Cu alloys. It is also observed in Figure 4 a good approximation among the obtained experimental laws for Al-Cu alloys solidified in the horizontal and upward directions with the same Cu-solute content (3 and 6) wt.%Cu.

Microstructure evolution of hypoeutectic Al-Cu alloys during solidification can be divided in two stages: primary dendrite Al-phase formation (α-matrix) and the subsequent eutectic transformation with precipitation of the intermetallic compound Al_2Cu (q), being located between the interdendritic ramifications. The incorporation of Si in the eutectic matrix (Al_2Cu) of the binary Al-6wt.%Cu alloy develops the microstructure α-Al + Al_2Cu + Si. Figures 5 to 7 depicts some detailed images of the Al-6wt.%Cu and Al-6wt.%Cu-8wt.%Si alloys as-cast microstructure by SEM-EDS mapping, respectively, which can elucidate the features observed and discussed in present work. In Figures 5a, 6b and 7, the points 1, 2 and 3 indicate the place where microanalysis by SEM-EDS mapping have been carried out, and the arrows represent the microstructural phases present in the analyzed alloys. Figure 7 shows
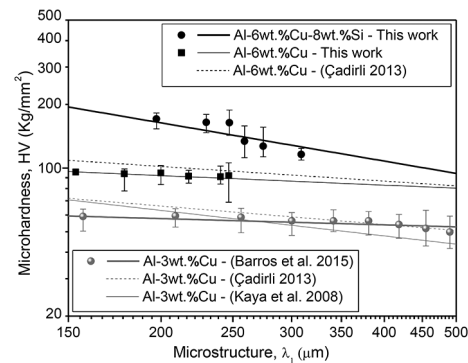
Figure 4 - Comparison of Hall-Petch experimental expressions obtained in this work and literature, according to Table I for Al-(3 and 6) wt.%Cu alloys.

a microanalysis on a Si particle. This has been obtained in SBU operation mode. In this case, the formed microstructure presents primary silicon particles dispersed in Al-rich-matrix, which appear to be responsible for the high hardness noted in Al-6wt.%Cu-8wt.%Si, according to the behavior seen in Figure 3.As reported previously in the introduction of this work, sufficient quantities of hard primary silicon particles are added in Al-Cu alloys to provide high wear resistance.

CONCLUSIONS

From the present experimental investigation with the Al-6wt.%Cu and Al-6wt.%Cu-8wt.%Si alloys samples, the following conclusions can be drawn:

For both studied alloys, the analysis of the microstructure indicated that the increasing of V_L and T_R reduced the primary dendrite arm spacing, increasing the microhardness. It was observed that a power law function characterizes the experimental variation of primary spacings with tip growth rate with an index of −1.1 as well as a −0.55 power law characterizes the experimental variation of primary spacings with cooling rate.

The microhardness dependency on the primary dendrite arm spacing can be represented by power type relationships given by HV = 204$(\lambda_1)^{-0.15}$ for Al-6wt.%Cu alloy and HV = 3926$(\lambda_1)^{-0.6}$ for Al-

6wt.%Cu-8wt.%Si alloy, respectively. As can be seen from the obtained relationships, the Hall-Petch exponent and slope values were higher in the analyzed ternary alloy. It was observed that the exponent value (0.15) found for the Al-6wt.% Cu alloy of this study is in good agreement with the values (0.098 and 0.12) obtained by Barros et al. (2015) for the Al-3wt.%Cu Al and Al-8wt.% Cu

(a)

(b)

	Weight (%)	
Points	Al	Cu
pt1	51.5	48.5
Pt2	94.2	5.8

(c)
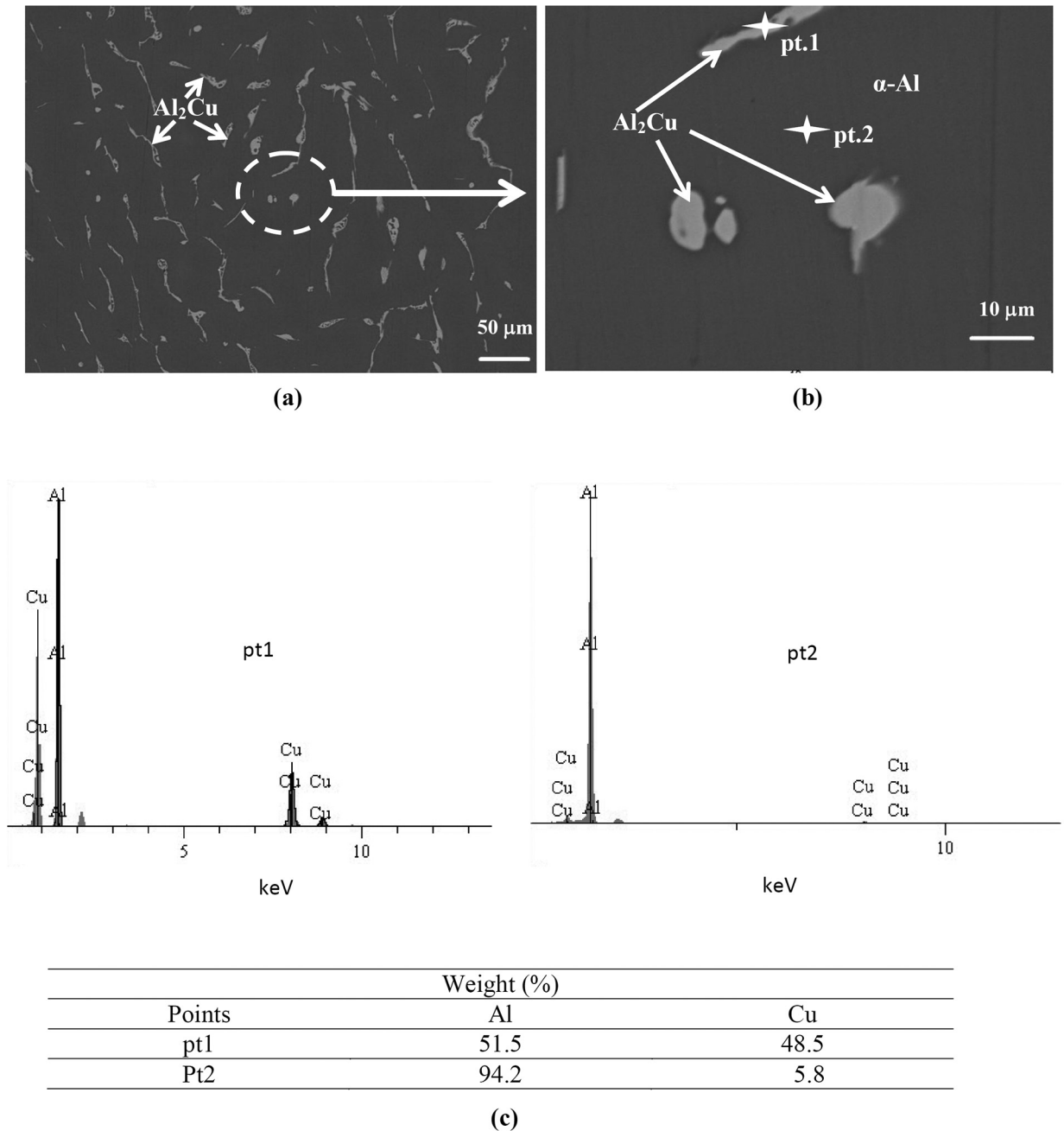
Figure 5 - Typical SEM micrograph and EDAX patterns of a Al-6wt.%Cu alloy sample at 40 mm (V_L = 0.28 mm/s T_R = 0.87 K/s and λ_1 = 235.9 µm) from the cooled surface of the casting for Al-6wt.%Cu alloy: **(a)** Accelerating Voltage: 20 kV; and Magnification: 200; **(b)** Accelerating Voltage: 20 kV and Magnification: 1500; **(c)** EDAX patterns and the corresponding chemical composition.

(a)   **(b)**
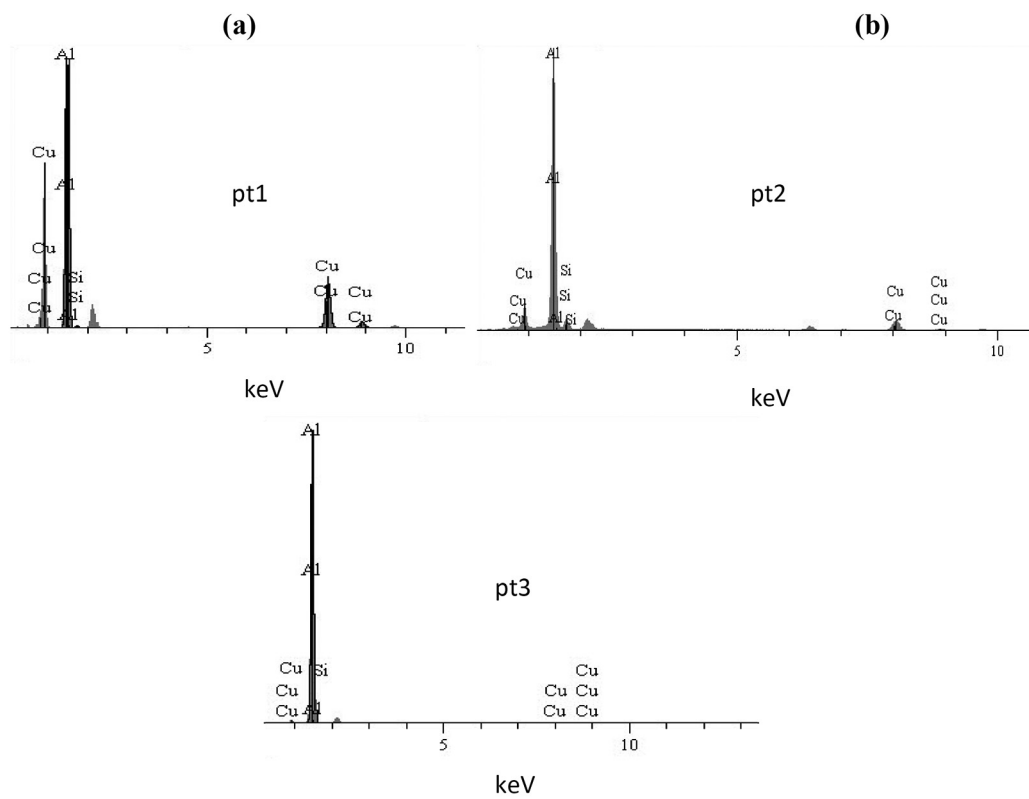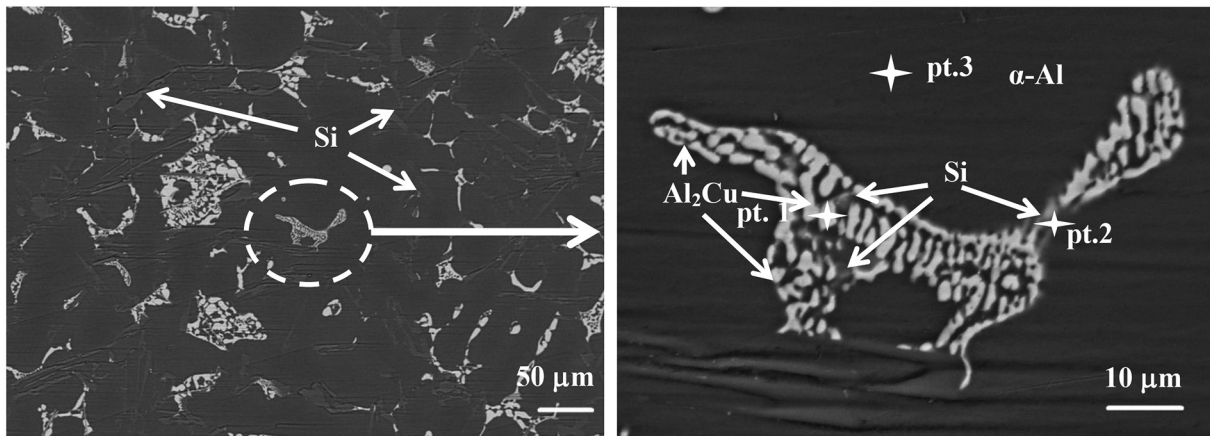
Weight (%)			
Points	Al	Cu	Si
pt1	61.0	36.7	2.3
pt2	75.0	19.0	6.0
pt3	94.1	5.5	0.4

(c)

Figure 6 - Typical SEM micrograph and EDAX patterns of a Al-6wt.%Cu-8wt.%Si alloy sample at 40 mm (V_L = 0.33 mm/s, T_R = 0.91 K/s and λ_1 = 302.3 µm) from the cooled surface of the casting for Al-6wt.%Cu-8wt.%Si alloy: (**a**) Accelerating Voltage: 20 kV and Magnification: 200; (**b**) Accelerating Voltage: 20 kV and Magnification: 1500; (**c**) EDAX patterns and the corresponding chemical composition.

(a)

(b)
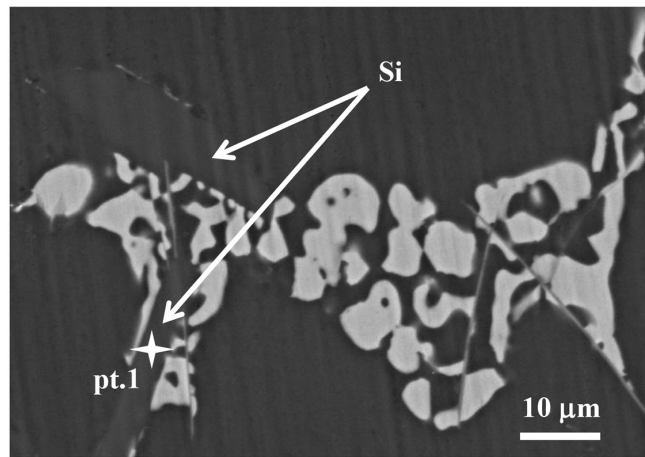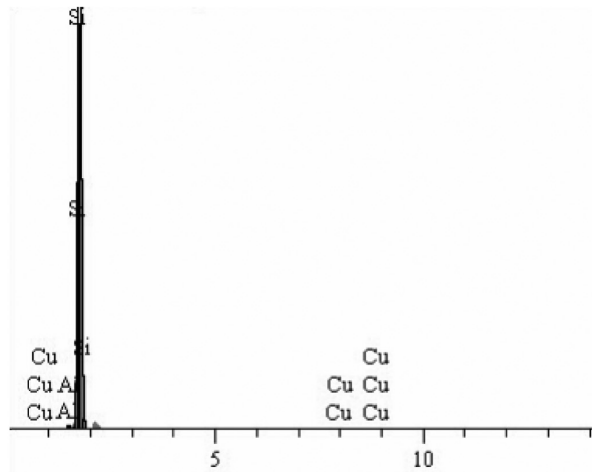
	Weight (%)		
Points	Al	Cu	Si
pt1	0.699	0.529	98.771

(c)

Figure 7 - Typical SEM micrograph and EDAX patterns of a Al-6wt.%Cu-8wt.%Si alloy sample at 70 mm (V_L = 0.28 mm/s, T_R = 0.71 K/s and λ_1 = 336.2 μm) from the cooled surface of the casting for Al-6wt.%Cu-8wt.%Si alloy: **(a)** Accelerating Voltage: 20 kV and Magnification: 200; **(b)** Accelerating Voltage: 20 kV and Magnification: 1500; **(c)** EDAX patterns and the corresponding chemical composition on a Si particle.

alloys, respectively. As seen from the comparison between the results of this work with the literature for steady-state upward solidification the exponent values 0.29, 0.23, 0.25, and 0.25 obtained by Çadirli (2013) for Al_{100-x}-Cu_x alloys (x=3 wt%, 6 wt%, 15 wt%, 24 wt%) are approximately two time larger than the value of 0.15 of this work, except for the value obtained for the alloy Al-33wt.%Cu, which was equal to of this work. It has also been noted that the exponent value (0.4) obtained by Kaya et

al. (2008) is approximately three times larger the value of this investigation (0.15).

From the comparative analysis between this work and the literature, for Al-Cu alloys solidified in the horizontal and upward directions, it has been also observed that the relationship obtained for the same Cu-solute content (3 and 6) wt.% Cu, has provide a good approximation between the Hall-Petch-experimental expressions obtained for these alloys solidified in the horizontal and upward directions.

The incorporation of Si in Al-6wt.%Cu alloy to form the Al-6wt.%Cu-8wt.%Si alloy have influenced significantly the microstructure and consequently the microhardness, but did not affect the primary dendritic growth law, as noted, i.e., the formed microstructure presents primary silicon particles dispersed in Al-rich α-matrix that appear to be responsible for the high hardness observed in Al-6wt.%Cu-8wt.%Si alloy.

Finally, this study may contribute to a better understanding of the thermal parameters and processes occurred in the Al-Cu and Al-Cu-Si alloys during solidification. The achieved results can be applied for liquid metal processing in science and industry aiming at designing of a required microstructure and mechanical properties of these alloys.

RESUMO

Um estudo experimental foi realizado para avaliar a evolução da microestrutura e da microdureza nas ligas binária Al-6% Cu e multicomponente Al-6%Cu-8%Si solidificadas direcionalmente e o efeito do elemento de liga Si. Para tanto, espécimes das ligas Al-6%Cu e Al-6%Cu-8%Si foram preparadas e solidificadas em condições transitórias de extração de calor. Um dispositivo de solidificação direcional horizontal refrigerado a água foi utilizado. Uma adequada caracterização é realizada, incluindo as velocidades experimentais de deslocamento da *isoterma liquidus* (V_L), taxas de resfriamento (T_R), medições de microdureza (HV), microscopias óptica e eletrônica de varredura com microanálise realizada por espectrometria de energia dispersiva (MEV-EDS). Os resultados mostram que, para ambas as ligas estudadas, os aumentos de V_L e T_R reduziram o espaçamento dendrítico primário, aumentando a microdureza. Além disso, a adição de Si na liga Al-6%Cu, para formar a liga Al-6%Cu-8%Si, influenciou significativamente a microestrutura e, consequentemente, a microdureza, não afetando, contudo, a lei de crescimento dendrítico primário. Uma análise sobre a formação da transição colunar/equiaxial (TCE) foi também realizada e os resultados mostram que a TCE não ocorre em um único plano, isto é, a TCE, em ambos os casos, ocorre em uma zona, que não é paralela à chapa molde refrigerada, onde ambos grãos colunares e equiaxiais coexistem.

Palavras-chave: solidificação, metais e ligas, microscopia eletrônica, dureza.

REFERENCES

ATWOOD RC AND LEE PD. 2003. Simulation of the three-dimensional morphology of solidification porosity in an aluminium-silicon alloy. Acta Mater 51: 5447-5466.

BARROS AS, MAGNO IL, SOUZA FA, OTA CA, MOREIRA AL, SILVA MA AND ROCHA OL. 2015. Measurements of microhardness during transient horizontal directional solidification of Al-rich Al-Cu alloys: effect of thermal parameters, primary dendrite arm spacing and Al₂Cu intermetallic phase. Met Mater Int 21: 429-439.

ÇADIRLI E. 2013. Effect of solidification parameters on mechanical properties of directionally solidified Al-rich Al-Cu alloys. Met Mater Int 19:411-422.

ÇADIRLI E AND GÜNDÜZ M. 2000. The directional solidification of Pb-Sn alloys. J Mater Sci 35: 3837-3848

CARVALHO DB, GUIMARÃES EC, MOREIRA AL, MOUTINHO DJ, FILHO JMD AND ROCHA OL. 2013. Characterization of the Al-3wt.%Si alloy in unsteady-state horizontal directional solidification. Mater Res 16: 874-883.

COSTA TA, MOREIRA AL, MOUTINHO DJ, DIAS M, FERREIRA IL, SPINELLI JE, ROCHA OL AND GARCIA A. 2015.

Growth direction and Si alloying affecting directionally solidified structures of Al-Cu-Si alloys. Mater Sci Techol 31: 1103-1112.

EASTON M, DAVIDSON C AND JOHN D. 2010. Effect of alloy composition on the dendrite arm spacing of multicomponent aluminum alloys. Metall Mater Trans A 41: 1528-1538.

EMMA S AND SALEM S. 2010. The heat treatment of Al-Si-Cu-Mg casting alloys. J Mater Process Technol 210: 1249-1259.

FERREIRA IL, LINS JFC, MOUTINHO DJ, GOMES LG AND GARCIA A. 2010. Numerical and experimental investigation of microporosity formation in a ternary Al-Cu-Si alloy. J Alloys Compd 503: 31-39.

GOMES LG, MOUTINHO DJ, FERREIRA IL, ROCHA OL AND GARCIA A. 2015. The growth of secondary dendritic arms in directionally solidified Al-Si-Cu alloys: a comparative study with binary Al-Si alloys. Appl Mech Mater 719-720: 102-105.

GOULART PR, SPINELLI JE, CHEUNG N AND GARCIA A. 2010. The effects of cell spacing and distribution of intermetallic fibers on the mechanical properties of hypoeutectic Al-Fe alloys. Mater Chem Phys 119: 272-278.

HARO S, RAMÍREZ J, DWIVEDI DK AND MARTÍNEZ E. 2009. Influence of solutionising and aging temperatures on microstructure and mechanical properties of cast Al-Si-Cu alloy. Mater Sci Technol 25: 886-891.

KAYA H, BÖYÜK U, ÇADIRLI E AND MARASLI N. 2012. Measurements of the microhardness, electrical and thermal properties of the Al-Ni eutectic alloy. Mater Des 34: 707-712.

KAYA H, ÇADIRLI E, BÖYÜK U AND MARASLI N. 2008. Variation of microindentation hardness with solidification and microstructure parameters in the Al based alloys. Appl Surf Sci 255: 3071-3078.

POLMEAR IJ. 2006. Light alloys: from traditional alloys to nanocrystals, 4th ed., Oxford: Butterworth-Heinemann, 416 p.

QUARESMA JMV, SANTOS CA AND GARCIA A. 2000. Correlation between unsteady-state solidification conditions, dendrite spacings, and mechanical properties of Al-Cu alloys. Metall Mater Trans A 31: 3167-3178.

RAPPAZ M AND BOETTINGER WJ. 1999. On dendritic solidification of multicomponent alloys with unequal liquid diffusion coefficients. Acta Mater 47: 3205-3219.

ROCHA OL, SIQUEIRA CA AND GARCIA A. 2003. Heat flow parameters affecting dendrite spacings during unsteady-state solidification of Sn-Pb and Al-Cu alloys. Metall Mater Trans A 34: 995-1006.

ROOY EL. 1990. Properties and selection: nonferrous alloys and special-purpose materials. In: Metals Handbook, Materials Park: ASM International, Ohio, USA, p. 490-539.

SADROSSADAT SM AND JOHANSSON S. 2010. The effects of solidification conditions and heat treatment on the microstructure and mechanical properties of EN-AC 44400 alloy. Mater Sci Forum 649: 505-510.

SILVA JN, MOUTINHO DJ, MOREIRA AL, FERREIRA IL AND ROCHA OL. 2009. The columnar to equiaxed transition during the horizontal directional solidification of Sn-Pb alloys. J Alloys Compd 478: 358-366.

SILVA JN, MOUTINHO DJ, MOREIRA AL, FERREIRA IL AND ROCHA OL. 2011. Determination of heat transfer coefficients at metal-mold interface during horizontal unsteady-state directional solidification of Sn-Pb alloys. Mater Chem Phys 130: 179-185.

SWAMINATHAN CR AND VOLLER VR. 1997. Towards a general numerical method for analysis of solidification systems. Int J Heat Mass Transf 40: 2859-2868.

VOLLER VR. 1998. A numerical scheme for solidification of an alloy. Can J Met Quart 37: 169-177.